

(Super)Gelators derived from push-pull chromophores: Synthesis, gelling properties and second harmonic generation

A.Belén Marco,^a Denis Gindre,^b Konstantinos Iliopoulos,^b Santiago Franco,^a Raquel Andreu,^{*,a} David Canevet^{*,b} Marc Sallé^{*,a}

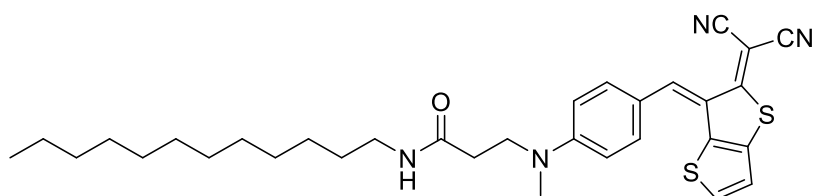
^a Departamento de Química Orgánica, ICMA, Universidad de Zaragoza-CSIC, 50009 Zaragoza, Spain.

^b Laboratoire MOLTECH-Anjou, Université d'Angers, UMR CNRS 6200, 2 bd Lavoisier, 49045 Angers Cedex, France.

Table S1 Tested conditions to synthesize chromophore 1	S2
Scheme S1 Chemical structure of the regioisomer of gelator 1 .	S2
Table S2 Solvents under consideration for the gelation studies and their Hansen solubility parameters.	S2
Fig. S1 Solubility data for compounds 1' (left) and 2 (right) in the Hansen space.	S3
Fig. S2 Projection of the Hansen space according to the δ_d axis with solubility data for gelator 2 .	S3
Fig. S3 Optical micrographs of 1' -based xerogels prepared from the different gelled solvents.	S4
Fig. S4 Optical micrographs of 2 -based xerogels prepared from the different gelled solvents.	S5
Fig. S5 Scanning electron micrographs obtained from 1' -based xerogels prepared from <i>o</i> -dichlorobenzene (left) and chloroform (right).	S5
Fig. S6 Optical micrographs of a 1' -based xerogels prepared from 1,2,4-trichlorobenzene with non-polarized (left) and polarized light (right).	S6
Fig. S7 Optical micrographs of 1' -based xerogels obtained from 1,2,4-trichlorobenzene (left – non-polarized light) and acetonitrile (right – polarized light).	S6
Fig. S8 Schematic representation of the modified second harmonic generation microscope.	S7
Table S3 Optical and SHG micrographs of the xerogels prepared from 1' .	S8
Table S4 Optical SHG micrographs of the xerogels prepared from 2 .	S9
Fig. S9 Effect of the polarization over the SHG response of xerogels-based microstructures derived from organogelator 1' .	S10
Collection of NMR spectra	S11

Table S1 Tested conditions to synthesize chromophore **1**.

Ac ₂ O, reflux	Complex mixture (1 not detected)
EtOH, NEt ₃ , reflux	Complex mixture (1 not detected)
EtOH, r.t.	Grafting on position 3 (cf Scheme 5)
AcOH, NEt ₃ , reflux	Complex mixture (1 not detected)
CHCl ₃ , silica, microwaves	Grafting on position 3 (cf Scheme 5)

**Scheme S1** Chemical structure of the regioisomer of gelator **1**.**Table S2** Solvents under consideration for the gelation studies and their Hansen solubility parameters.

Solvents	δ_d	δ_H	δ_p
1,2-Dichlorobenzene	19.2495	3.3005	6.314
Acetonitrile	15.334	6.109	18.04
Chlorobenzene	19.0445	2.009	4.305
Toluene	18.04	2.009	1.394
Acetone	15.5	7	10.4
1,2,4-Trichlorobenzene	20.2	3.2	6
<i>p</i> -Xylene	17.6	3.1	1
1,4-Dioxane	19	7.4	1.8
Octan-1-ol	17	11.9	3.3
Chloroform	17.835	5.7195	3.116
Ethyl acetate	15.826	7.216	5.3095
1,1,2,2-Tetrachloroethane	18.8	5.3	5.1
Tetrachloromethane	17.835	0.5945	0
Hexane	14.92	0	0
Cyclohexane	16.8305	0.205	0
Tetrahydrofuran	16.8305	8.0155	5.7195
Methanol	15.129	22.345	12.3205
Ethanol	15.826	19.434	8.815
Propan-2-ol	15.826	16.441	6.109

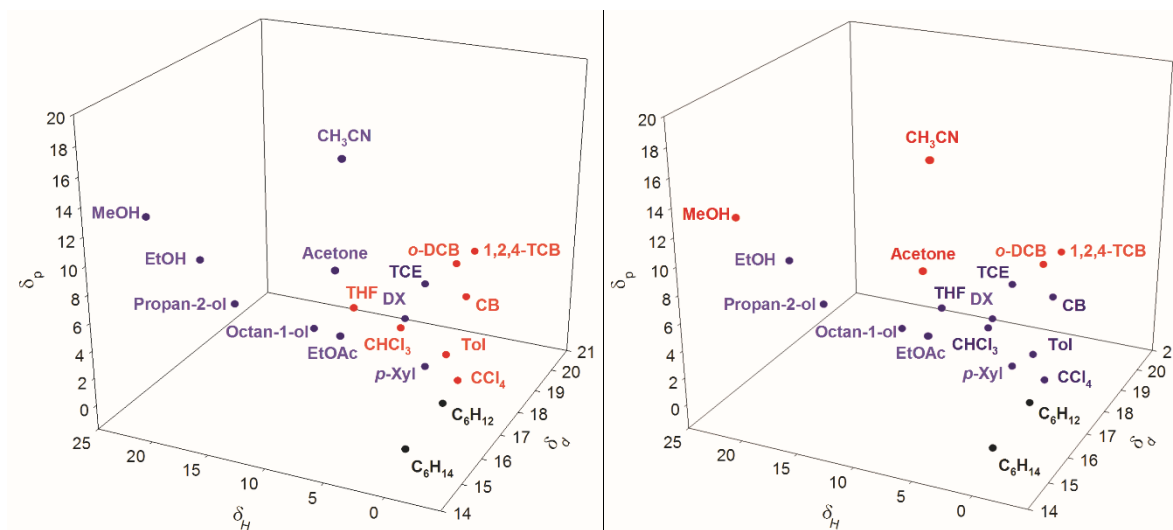


Fig. S1 Solubility data for compounds **1'** (left) and **2** (right) in the Hansen space. Red for gelation, blue for precipitation, black for insoluble at high temperatures.

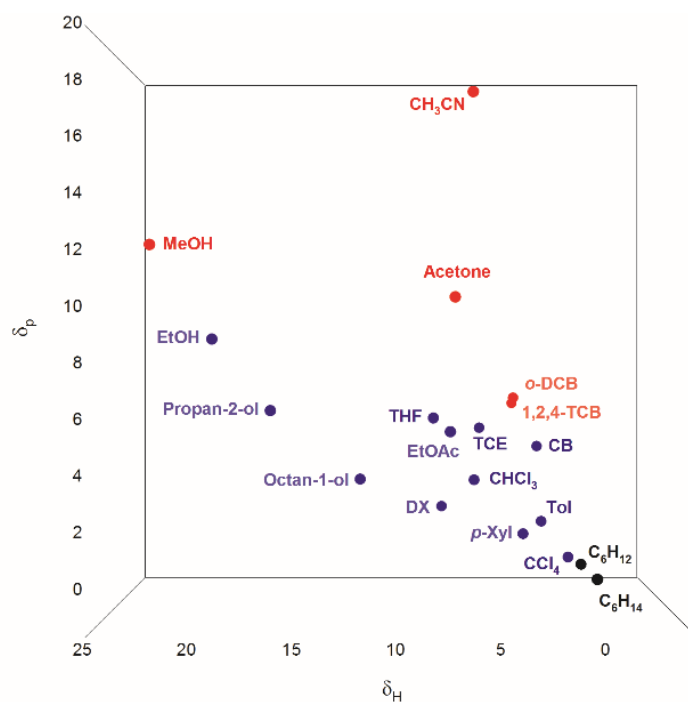


Fig. S2 Projection of the Hansen space according to the δ_d axis with solubility data for gelator **2**. Red for gelation, blue for precipitation, black for insoluble at high temperatures.

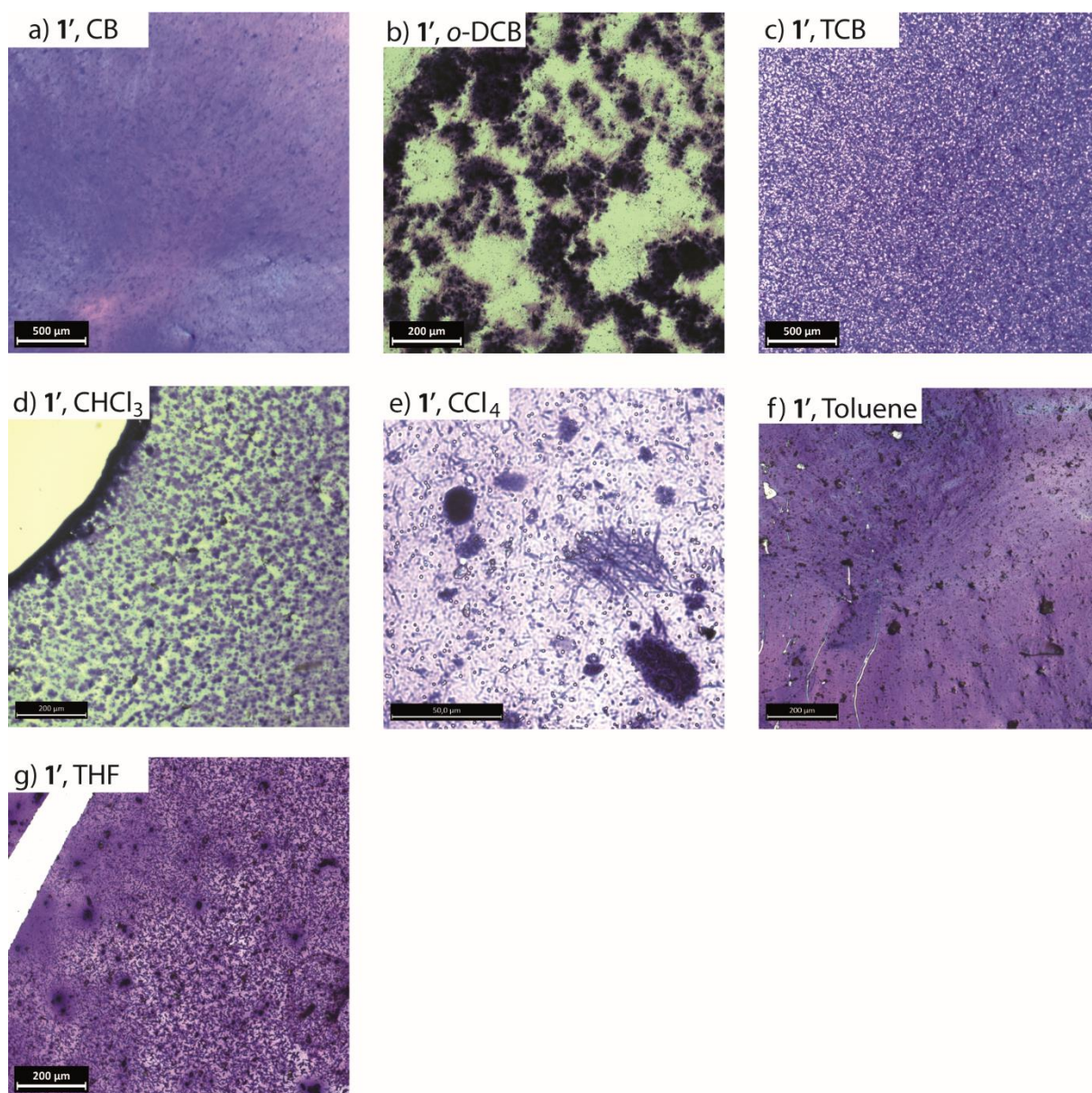


Fig. S3 Optical micrographs of 1'-based xerogels prepared from the different gelled solvents.

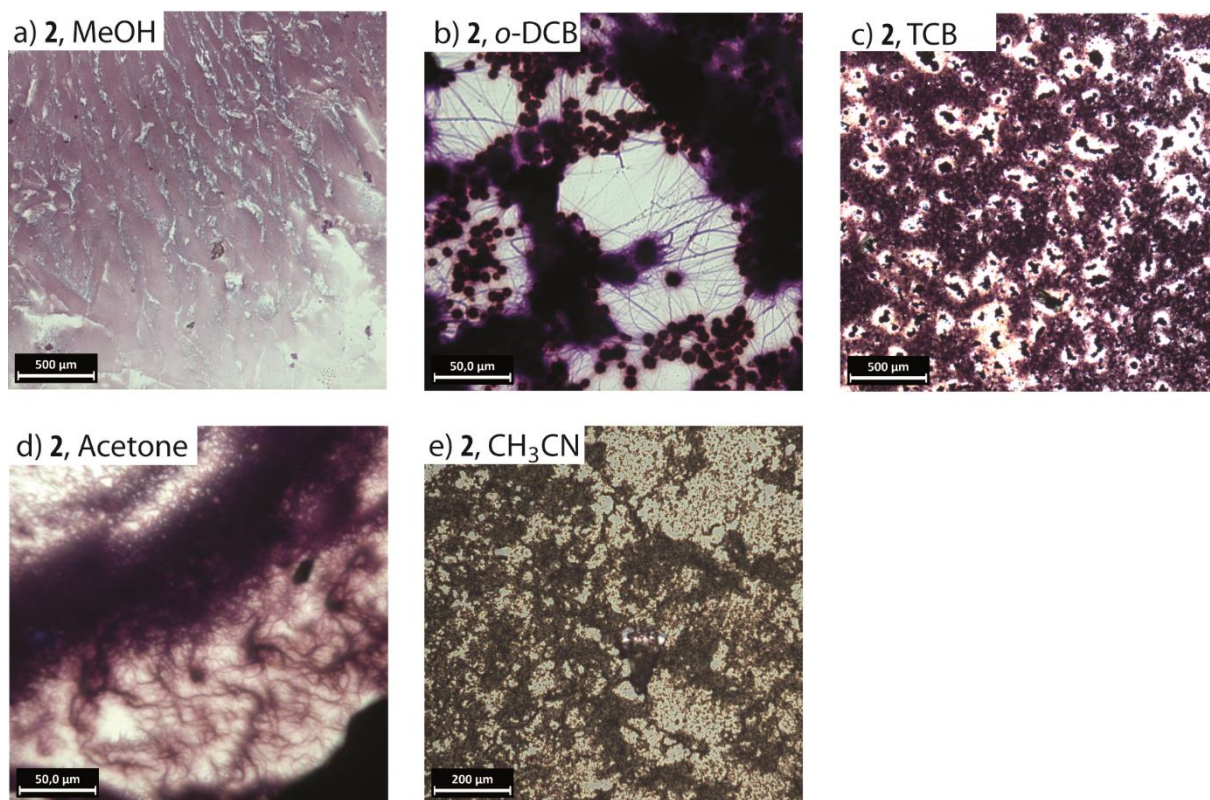


Fig. S4 Optical micrographs of **2**-based xerogels prepared from the different gelled solvents.

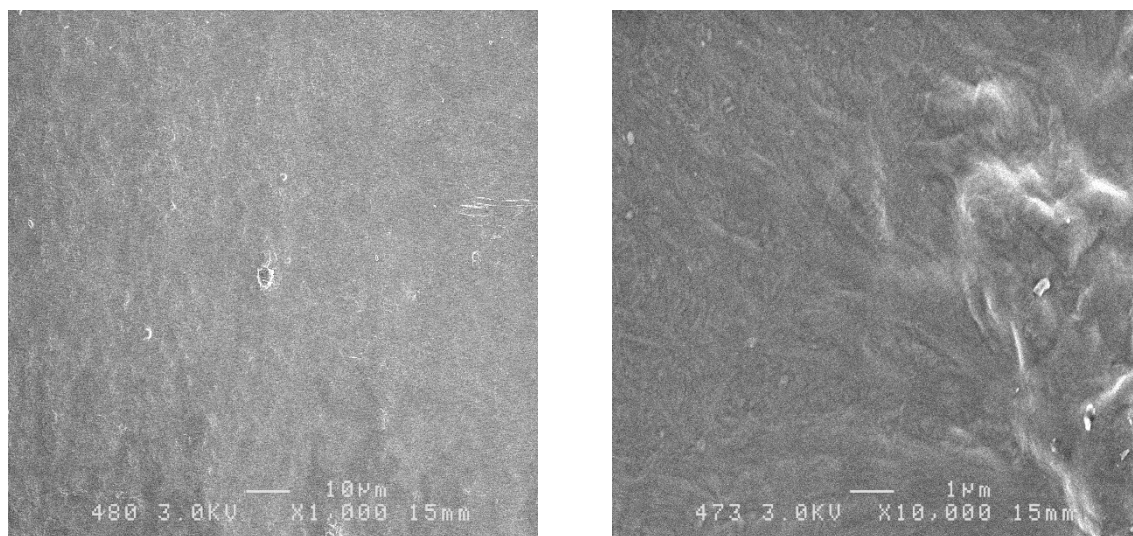


Fig. S5 Scanning electron micrographs obtained from **1'**-based xerogels prepared from o-dichlorobenzene (left) and chloroform (right).

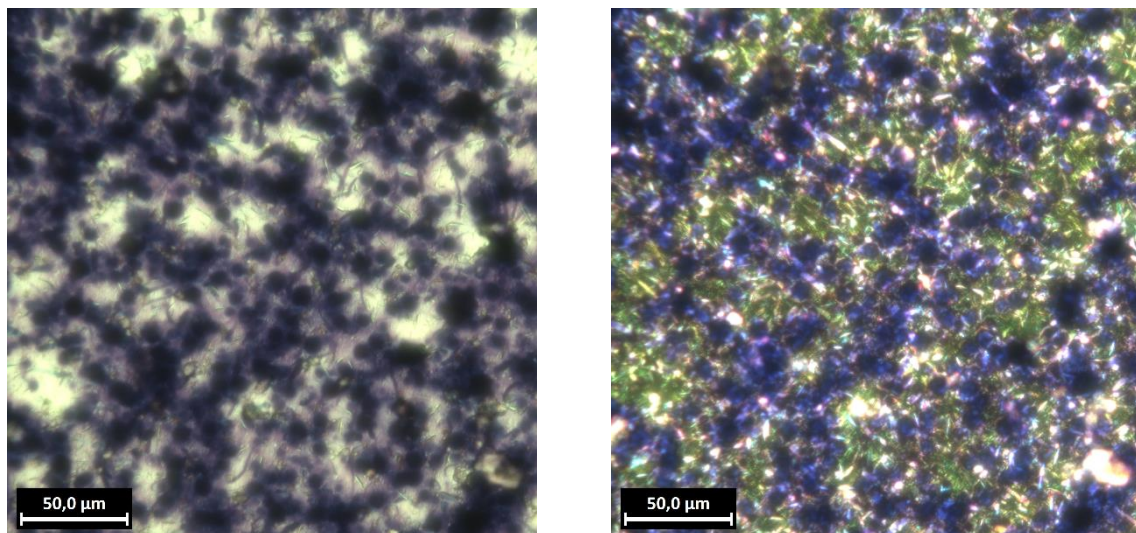


Fig. S6 Optical micrographs of a **1'**-based xerogels prepared from 1,2,4-trichlorobenzene with non-polarized (left) and polarized light (right). Both images correspond to the same region.

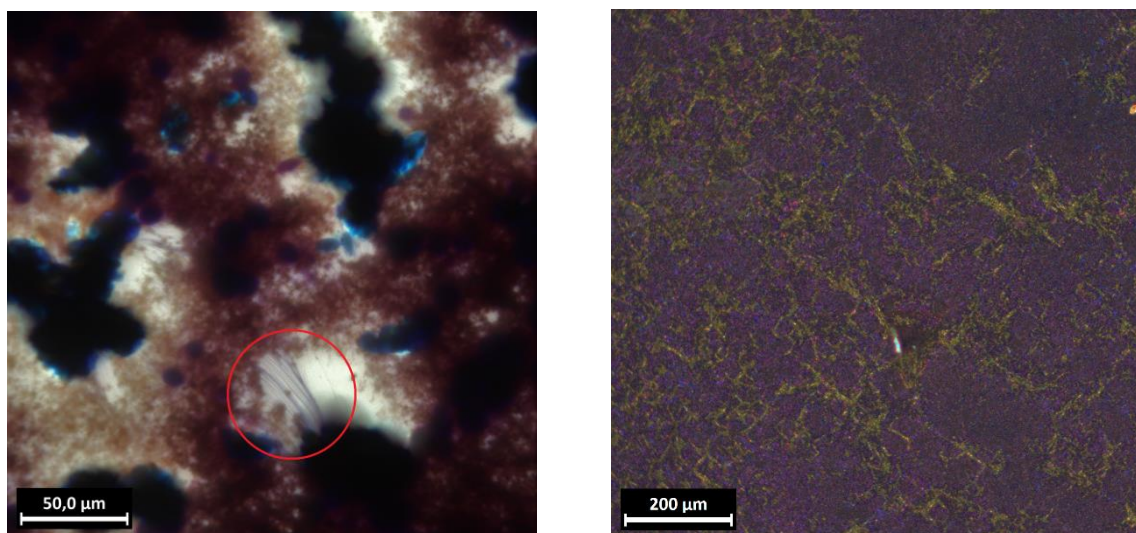


Fig. S7 Optical micrographs of **2**-based xerogels obtained from 1,2,4-trichlorobenzene (left – non-polarized light) and acetonitrile (right – polarized light).

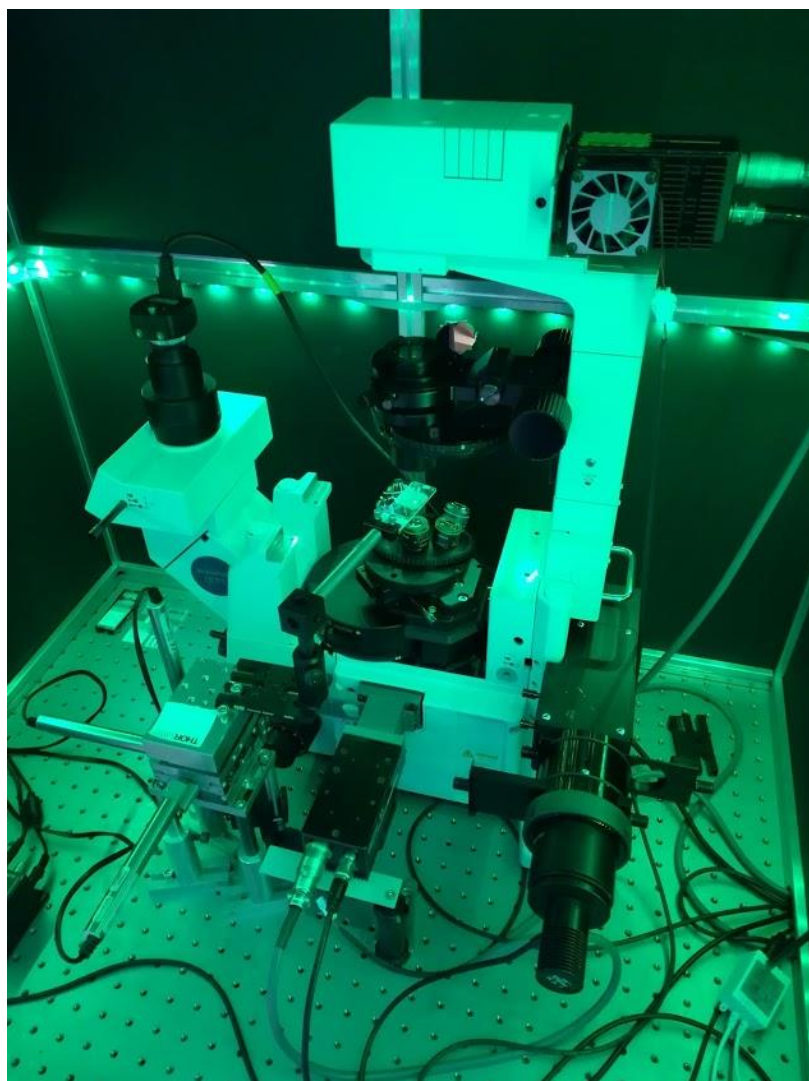
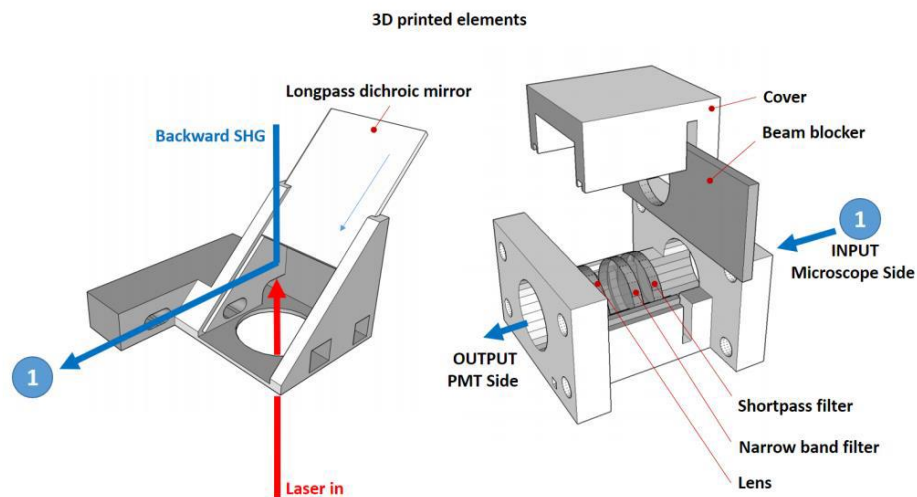


Fig. S8 Schematic representation of the modified second harmonic generation microscope and a picture of the whole device.

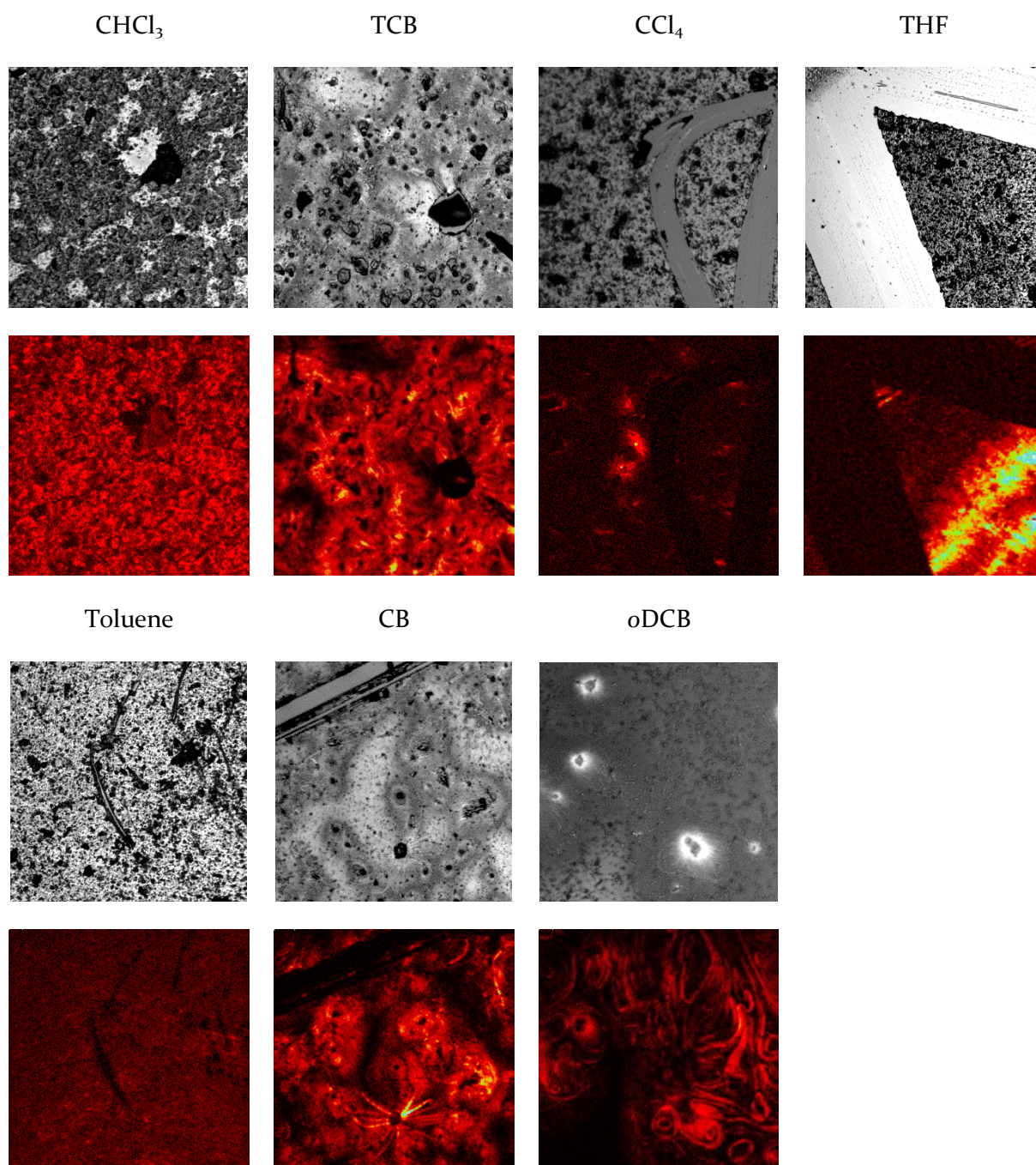


Table S3 Optical and SHG micrographs of the xerogels prepared from **1'**. These images have the same scale and are 360 μm wide.

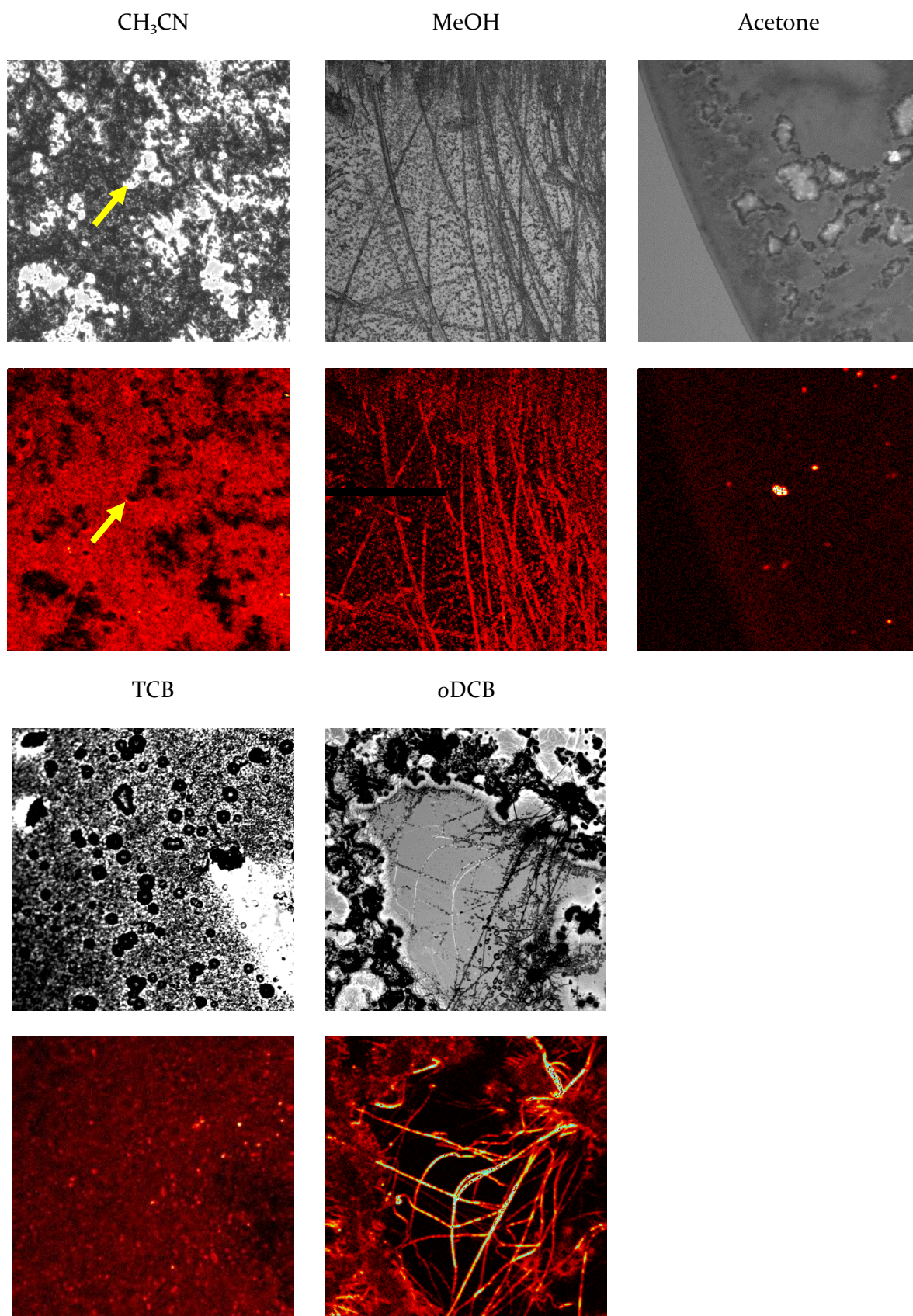


Table S4 Optical SHG micrographs of the xerogels prepared from **2**. These images have the same scale and are 360 μm wide. The yellow arrows highlight the same area of the sample prepared with acetonitrile.

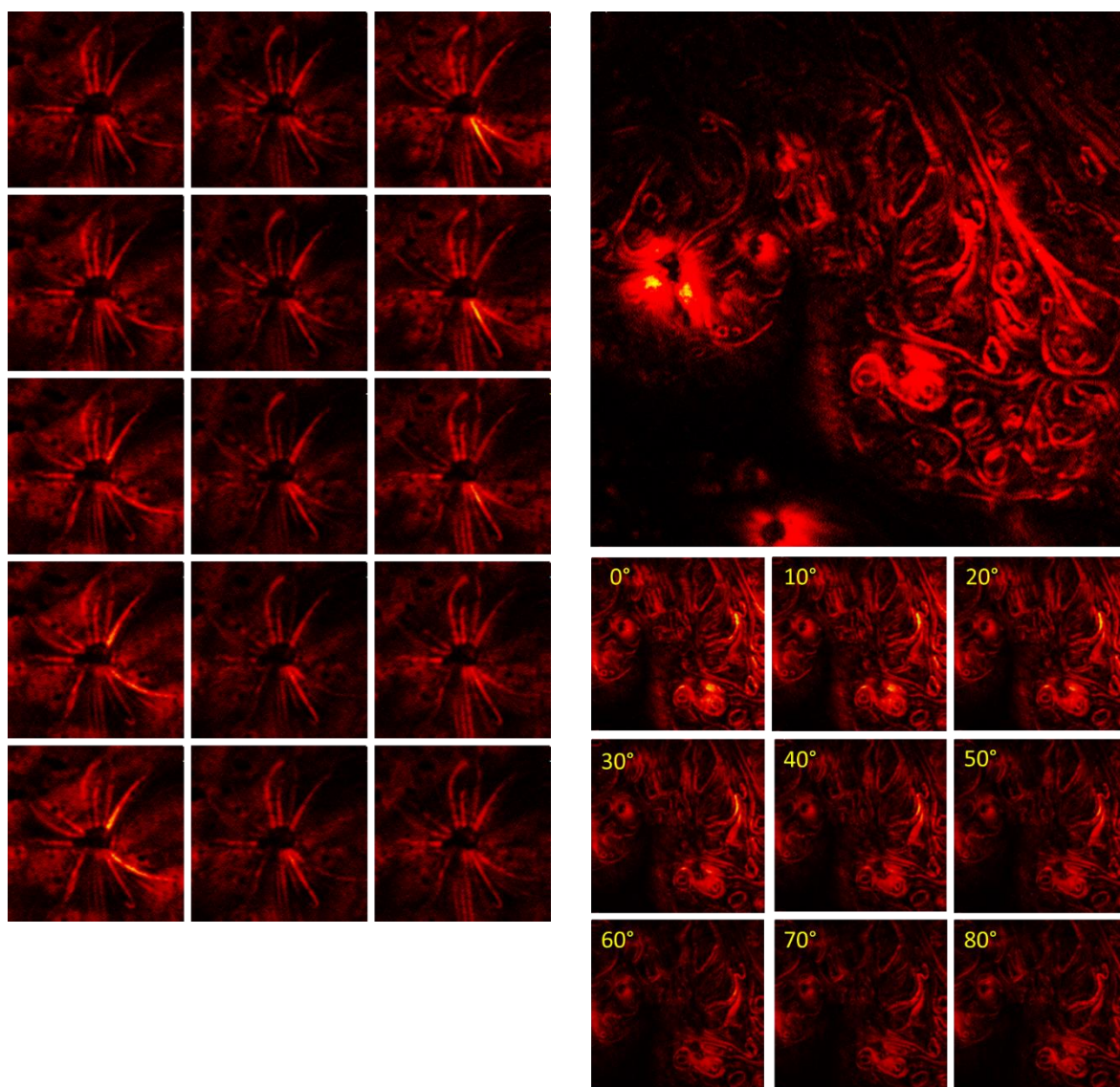
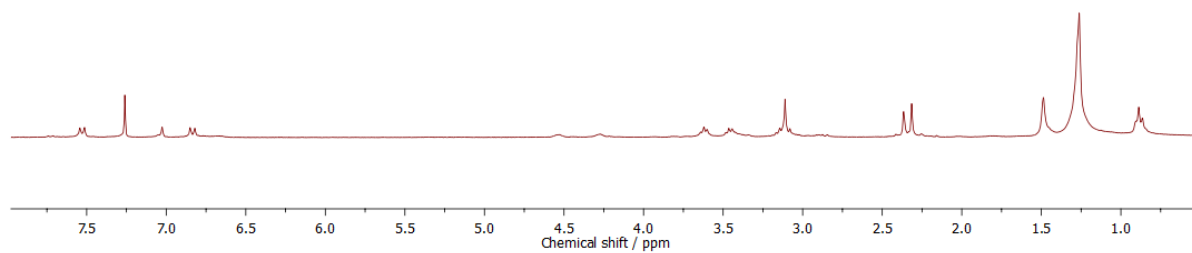
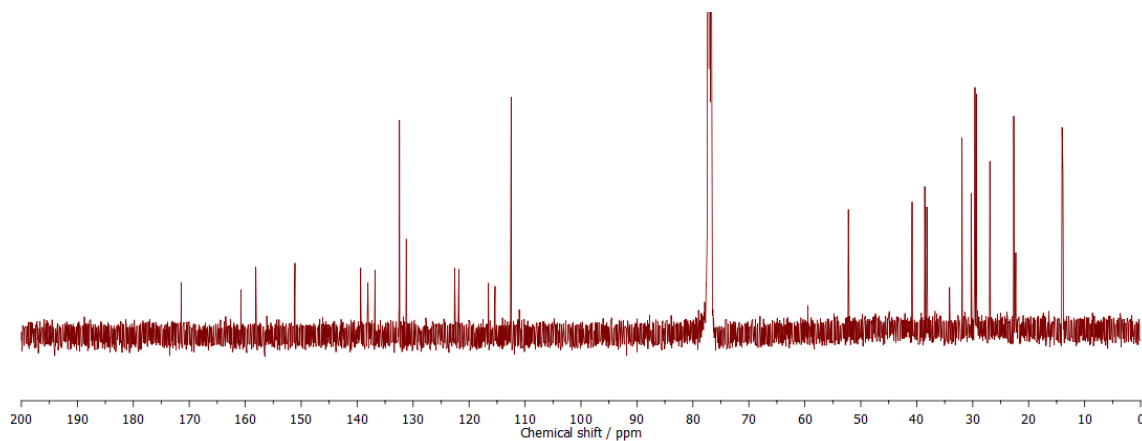


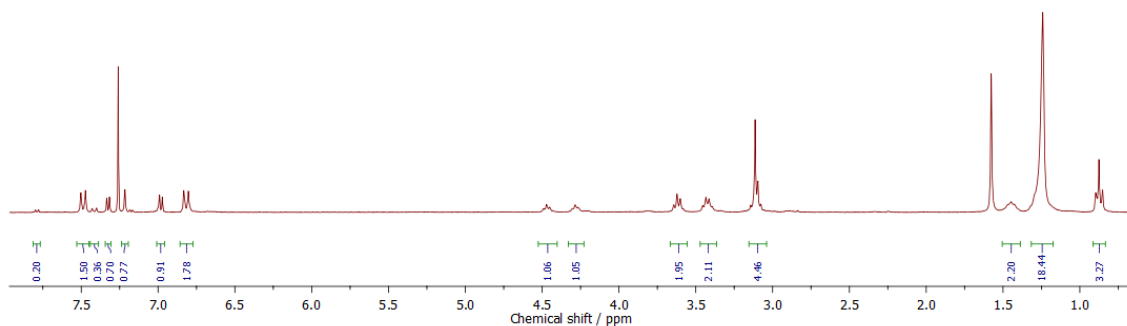
Fig. S9 Effect of the polarization over the SHG response of xerogels-based microstructures derived from organogelator **1**.



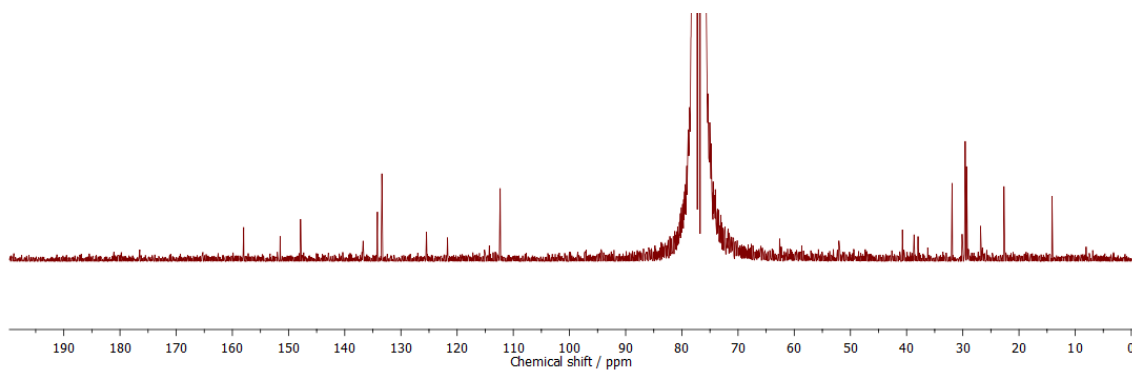
^1H NMR spectrum of gelator **1'**, CDCl_3 , 300 MHz



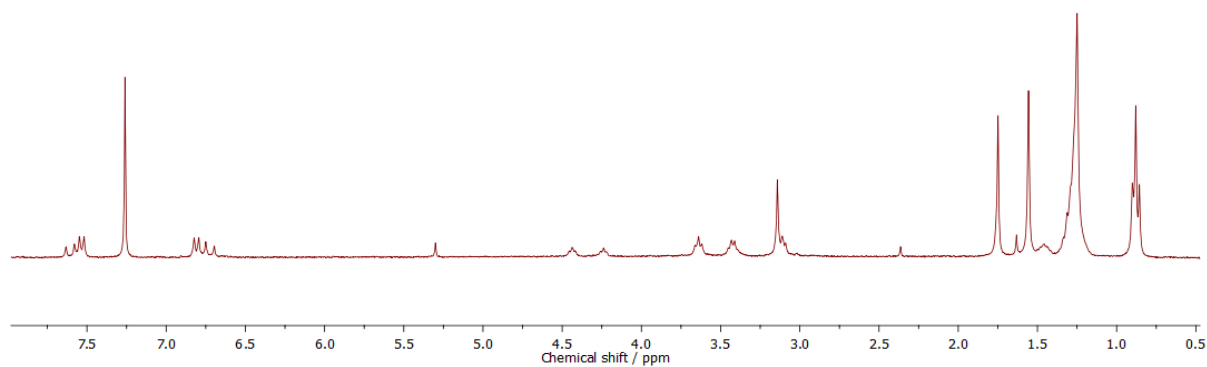
^{13}C NMR spectrum of gelator **1'**, CDCl_3 , 125 MHz, 323 K



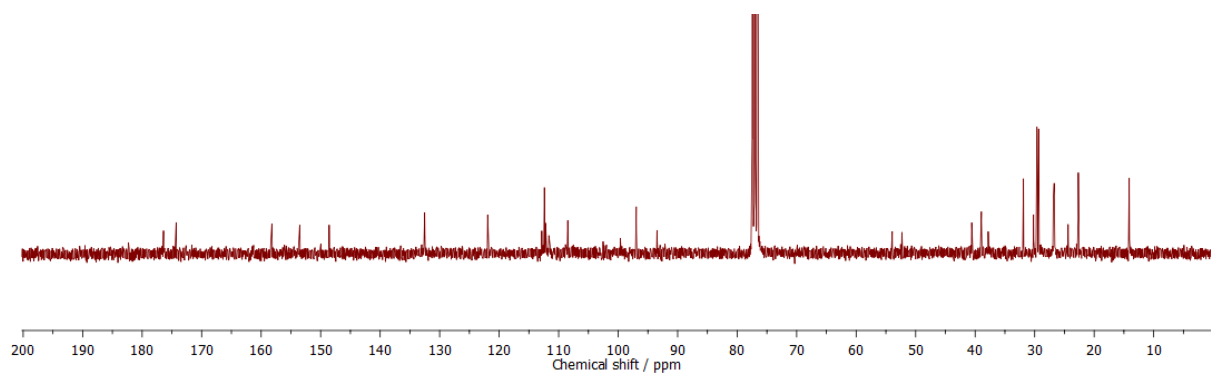
^1H NMR spectrum of gelator **2**, CDCl_3 , 300 MHz



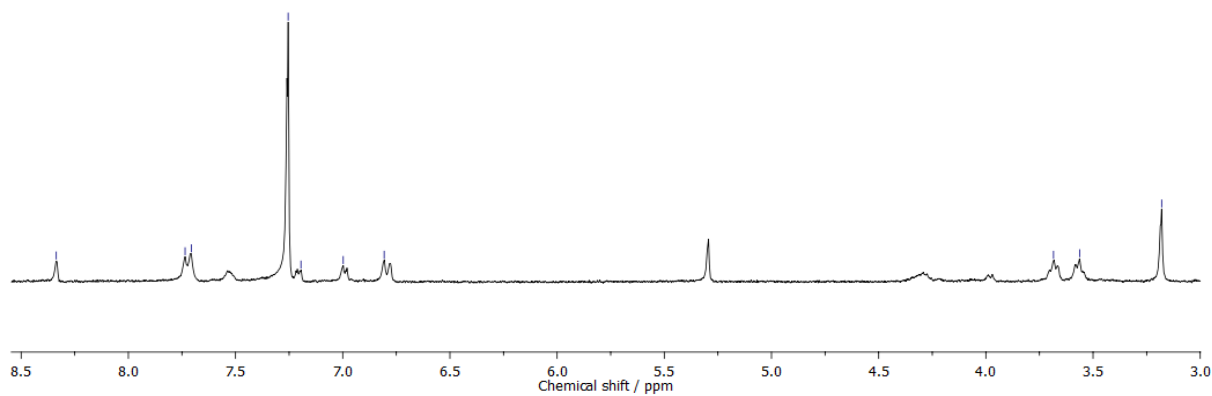
^{13}C NMR spectrum of gelator **2**, CDCl_3 , 75 MHz (Power phase correction of the MestReNova software)



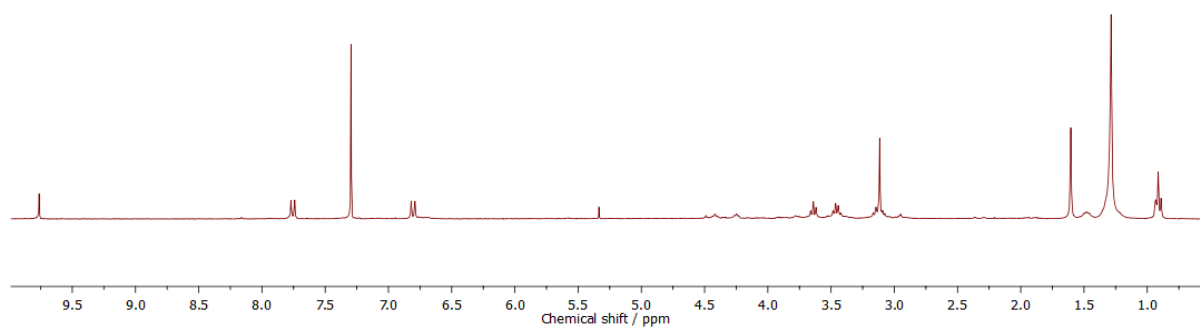
^1H NMR spectrum of compound **3**, CDCl_3 , 300 MHz



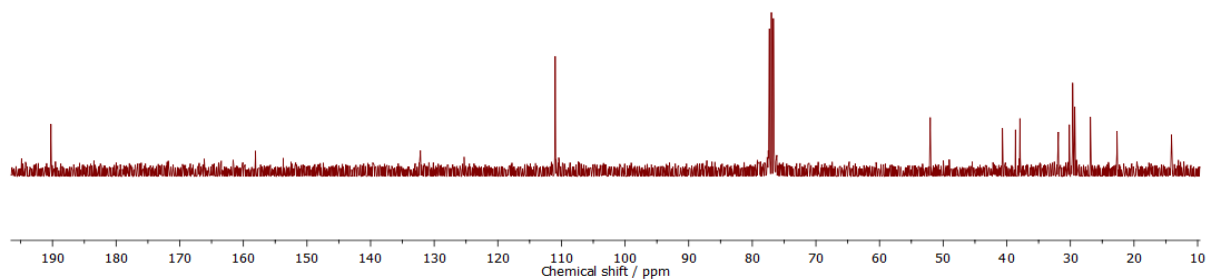
^{13}C NMR spectrum of compound **3**, CDCl_3 , 75 MHz



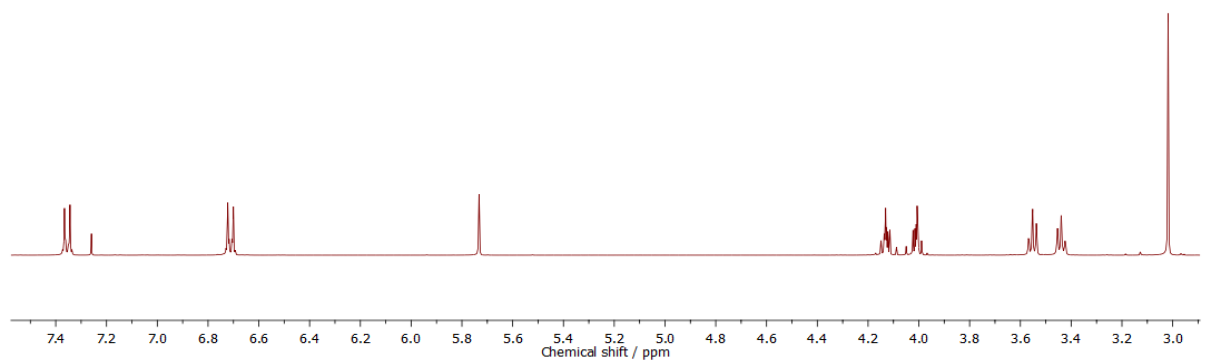
^1H NMR spectrum of azide **6**, CDCl_3 , 300 MHz



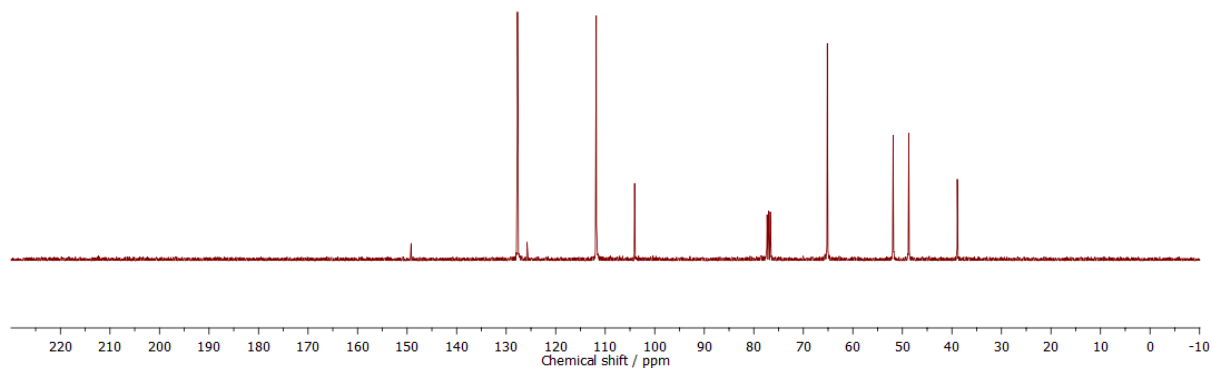
^1H NMR spectrum of aldehyde **7**, CDCl_3 , 300 MHz



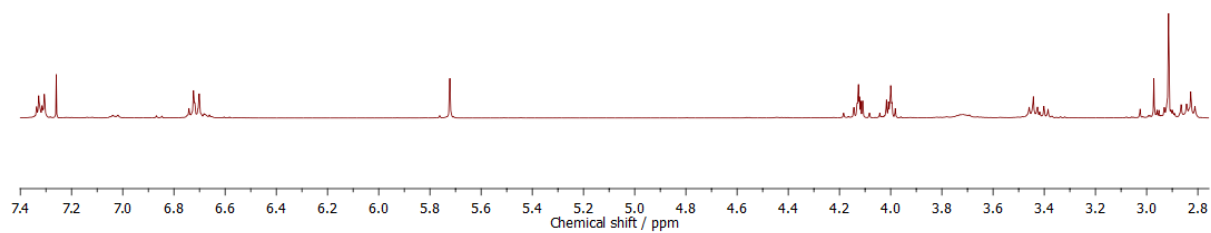
^{13}C NMR spectrum of aldehyde **7**, CDCl_3 , 75 MHz (magnitude processing from the MestReNova software)



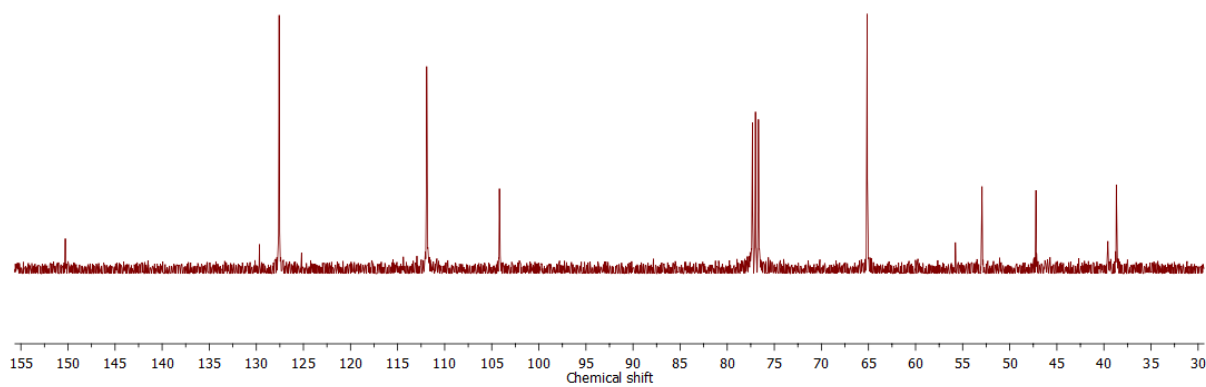
^1H NMR spectrum of azide **8**, CDCl_3 , 300 MHz



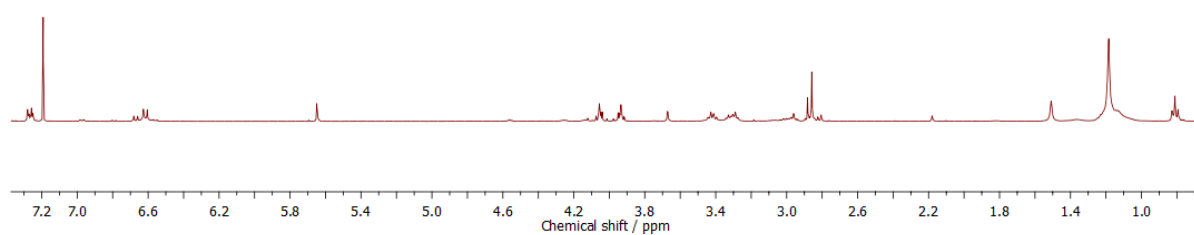
^{13}C NMR spectrum of azide **8**, CDCl_3 , 75 MHz (magnitude processing from the MestReNova software)



^1H NMR spectrum of amine **9**, CDCl_3 , 300 MHz



^{13}C NMR spectrum of amine **9**, CDCl_3 , 75 MHz



^1H NMR spectrum of urea **10**, CDCl_3 , 300 MHz